Insights Into the Uptake of N_2O_5 by Aqueous Aerosol Using Chemically Accurate Many-Body Potentials

Vinícius Wilian D. Cruzeiro,[1,2] Mirza Galib,[3] David T. Limmer,[3,4,5,6,a)] and Andreas W. Götz[1,b)]
[1)] *San Diego Supercomputer Center, University of California San Diego, La Jolla, California 92093*
[2)] *Department of Chemistry and Biochemistry, University of California San Diego, La Jolla, California 92093*
[3)] *Department of Chemistry, University of California, Berkeley, California*
[4)] *Kavli Energy NanoScience Institute, Berkeley, California*
[5)] *Materials Science Division, Lawrence Berkeley National Laboratory, Berkeley, California*
[6)] *Chemical Science Division, Lawrence Berkeley National Laboratory, Berkeley, California*

(Dated: 27 July 2021)

We study the uptake of N_2O_5 into pure water using molecular dynamics simulations performed with a recently developed, data-driven MB-nrg model. Our model follows the same basis of the MB-pol water many-body model and has coupled-cluster accuracy. We quantify the thermodynamics of solvation and adsorption using enhanced sampling techniques and free energy calculations. The free energy profile obtained highlights that N_2O_5 is selectively adsorbed to the liquid-vapor interface and weakly solvated. We further find that accommodation into the bulk solution occurs rather slowly, and competes with evaporation upon initial adsorption from the gas phase. The rates of each of these processes are evaluated using the free energy barriers and kinetically obtained fluxes. Leveraging the quantitative accuracy of the model, we parameterize and numerically solve a reaction-diffusion equation to determine a likely range of hydrolysis rates consistent with the experimentally observed reactive uptake coefficient in pure water. The physical and chemical parameters deduced here, including the solubility, accommodation coefficient, and hydrolysis rate, afford a foundation for which to consider the reactive loss of N_2O_5 in more complex solutions.

The uptake of trace gases from the air into aerosol particles impacts a wide range of environmental systems.[1,2] Among other things, such multiphase processes help to determine the oxidative power of the atmosphere by acting as sinks for nitrogen oxides.[3,4] Of particular long-standing interest is the reactive uptake of N_2O_5 in aqueous aerosol, which is estimated to account for 15-50% of the loss of NO_x in the troposphere.[5,6] Despite significant study, basic questions remain concerning the mechanism of N_2O_5 uptake.[7–13] Molecular dynamics simulations can be used to obtain a molecular perspective on gaseous uptake, free of underlying rate limitation assumptions.[14] However, studying such processes theoretically imposes challenges, since uptake coefficients are exponentially sensitive to free energy differences and the simulations involve large systems and long times to model the complex dynamics. While qualitative predictions of mechanisms can be typically studied with conventional empirical force fields or density functional theory based models,[13,15] quantitative predictions require higher levels of accuracy. Here we employ a recently developed many-body potential, MB-nrg,[16] to study the physical uptake of N_2O_5 into water, and infer its reactive uptake coefficient by solving a corresponding reaction-diffusion model. This MB-nrg potential has been parameterized from coupled-cluster calculations, and has the capability of making quantitative predictions of the thermodynamics and kinetics leading to the N_2O_5 uptake.

Gaseous uptake into fluid particles couples thermodynamic constraints of solubility with kinetic details of reaction and diffusion. As a complete analytical analysis of the appropriate reaction diffusion equations is not typically tenable, approximate models are commonly postulated employing a small number of thermodynamic and kinetic properties.[17] For example, the uptake of N_2O_5 in aqueous aerosol has been assumed to follow such a model, determined by bulk accommodation followed by bulk phase hydrolysis and parameterized by its bulk solubility and hydrolysis rate.[18] Such kinetic models typically lack molecular details, neglecting the finite width of the liquid-vapor interface and its potential unique properties. With molecular dynamics simulations these assumptions can be relaxed, and the relevant parameters extracted to inform an atomistic kinetic model.[19–21] Further, by solving the reaction diffusion equations numerically, the simplified models can be refined.

We apply this perspective to the reactive uptake of N_2O_5 as the validity of its kinetic model has been recently called into question. The reevaluation was prompted by the difficulty reconciling the traditional resistor model with field measurements, combined with theoretical work providing indications of interfacial stability and reactivity.[15,22] The mechanism of uptake has been recently explored directly using a neural network based reactive model, and it was found that interfacial rather than bulk phase processes dictate the observed uptake coefficient.[13] Using training data obtained from density functional theory, this study found that the hydrolysis rate was sufficiently fast at the interface that bulk phase partitioning cannot kinetically compete, and the uptake was determined by a competition between interfacial hydrolysis and evaporation. These calculations found mod-

[a)] Electronic mail: dlimmer@berkeley.edu
[b)] Electronic mail: agoetz@sdsc.edu

est agreement with experimental uptake coefficient values, consistent with the expected qualitative accuracy of the model employed. As direct experimental confirmation of the importance of the interface is difficult, an alternative means of validating it is to employ models with higher chemical accuracy. This is the aim of the current work.

MB-nrg potentials can serve to make quantitative prediction of gaseous uptake as they can be accurate yet computationally amenable to the large system sizes and long timescales required to simulate interfacial processes just like the MB-pol water model.[23,24] Contrary to common neural network models, these many-body potentials have an explicit representation for long-range interactions, which can be important at extended interfaces.[25] For example, it has been shown that MB-pol[26,27] yields quantitative accuracy for a variety of molecular properties across water's phase diagram.[26–43] Extensions of this modeling framework to describe mono-atomic ions and small molecules in aqueous solutions as well as generic mixtures of molecules have been recently realized.[44–48] These MB-nrg models include a model of N_2O_5 that has been developed using analogous approaches.[16] This MB-nrg model was demonstrated to yield comparable accuracy with respect to the coupled cluster reference data it was parameterized on, enabling highly accurate simulations of N_2O_5 in aqueous environments. While not able to describe reactions with water, the model nevertheless is capable of quantifying the processes that establish the physical uptake of N_2O_5, which can be subsequently combined with the reactive-diffusion models to make inferences regarding reactivity.

Here we employ the MB-nrg model with explicit one-body, two-body and three-body short-range interactions to simulate the uptake of N_2O_5 in water.[16] In order to extract the thermodynamic and kinetic properties that determine the uptake of N_2O_5, we have simulated a system containing a slab of liquid water in contact with its vapor and a single N_2O_5 molecule. The system is illustrated in Fig. 1A. The system is made up of 543 water molecules forming a liquid slab measuring 2.416 nm x 2.416 nm in cross-sectional area and 2.772 nm in length. The corresponding density profile of water along the direction perpendicular to the interface, $\rho(z)$, is shown in Fig. 1B, exhibiting the expected sinusoidal profile consistent with emergent capillary waves.[49] The bulk density of the MB-pol model ρ_B is 1.007 g/cm^3.[29] We take the origin of z to be coincident with the Gibbs dividing surface of the interface. The system is embedded in a simulation domain of the same cross-section and a length of 20 nm in order to accommodate periodic boundary conditions. Simulations are executed with Amber 2020[50] interfaced to the MBX[51] library. Ewald summation is employed to describe long-range electrostatics and dispersion interactions using a real-space cutoff of 1.2 nm. Thermodynamic averages are computed within an ensemble of fixed N particles, V volume, and $T = 300$ K temperature, using a Langevin thermostat and a timestep of 0.5 fs. Kinetic properties are evaluated within a constant energy ensemble with fixed N and V.

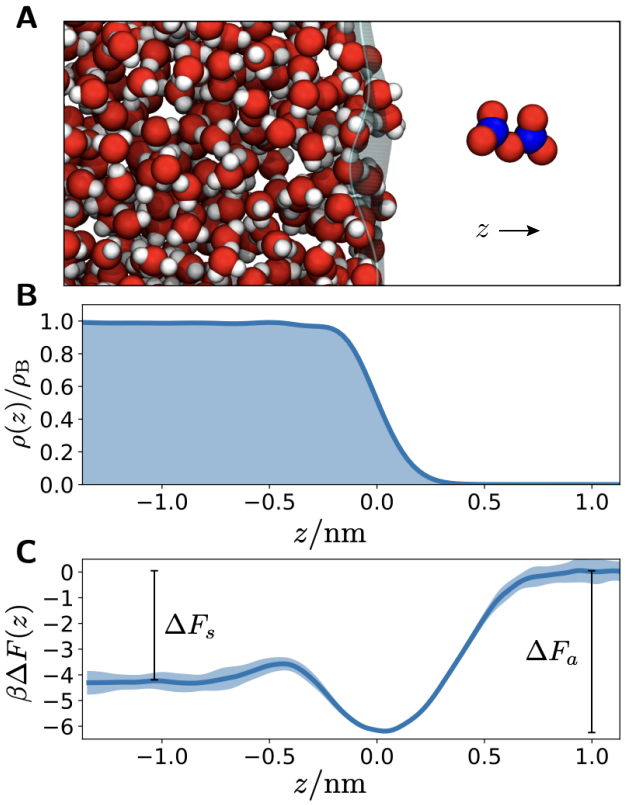

FIG. 1. Thermodynamics of N_2O_5 solvation. A) Characteristic snapshot of N_2O_5 near the water-vapor interface. B) Water density profile where $z = 0$ demarks the Gibbs dividing interface. C) Free energy to move N_2O_5 in the z direction, where the shaded region are one standard deviation error bars.

Using this simulation setup, we first considered the thermodynamics of N_2O_5 solvation in liquid water. We have computed the free energy to move a gaseous N_2O_5 into the liquid water slab using umbrella sampling applied to the center of mass distance along the z direction between the water slab and N_2O_5.[52] We employed harmonic biasing potentials of the form $\Delta U(z) = k/2(z - z^*)^2$ with a spring constant k of 2.5 kcal mol^{-1} A^{-2} and 52 independent windows with minima z^* spaced evenly between -1.36 and 1.19 nm. Three separate sets of calculations were run, each consisting of 1 ns equilibration time followed by 2.5 ns production time to compute partial histograms. The individual histograms from each window were combined using umbrella integration.[53]

Figure 1C shows the resulting average free energy profile obtained from the three independent simulations and the error bars are computed from the standard deviation for the three independent calculations[54]. For both $z \gg 0$ and $z \ll 0$, the free energy profile is flat, reflecting the translationally invariant bulk liquid and vapor on either side of the interface. We define the offset between these asymptotic values as $\beta\Delta F_s = -4.3 \pm 0.1$,

the solvation free energy for the gas phase N_2O_5, where $\beta = 1/k_BT$ and k_B is Boltzmann's constant. In between these two extremes, the free energy is non-monotonic and exhibits a global minimum approximately centered at the Gibb's dividing surface and a barrier to move the N_2O_5 molecule from this interfacial position into the bulk liquid. Relative to the gas phase, the global minimum corresponds to a favorable interfacial adsorption free energy of $\beta\Delta F_a = -6.2 \pm 0.1$. The globally favorable interfacial adsorption indicates N_2O_5 is relatively hydrophobic, consistent with previous observations of its relatively weak solvation.[13,15,55] This free energy profile dictates that the equilibrium density profile of N_2O_5 would be inhomogeneous in the vicinity of the liquid-vapor interface, a feature neglected in typical kinetic models.

From the free energy profile we can calculate the solubility of N_2O_5 in liquid water. In dilute solution at concentration c_l in contact with a solute with partial pressure p, this solubility is traditionally reported as a Henry's law constant defined as[56]

$$H = \frac{c_l}{p} = \beta e^{-\beta \Delta F_s} \tag{1}$$

and computable from the solvation free energy defined operationally from our free energy profile. This estimate gives a Henry's law constant $H = (3.0 \pm 0.4)$ M/atm. This value is in line with typical inferences from experiment, though its direct measurement is hindered by the facile hydrolysis of N_2O_5.[56,57] This value is higher than recent estimates employing fixed charge force fields and neural network potentials, each of which found a value closer to 0.5 M/atm.[13,15] We can also evaluate the mass accommodation coefficient, defined as the probability of a gas molecule to solvate into the bulk of the liquid from the interface. The mass accommodation coefficient, α, can be computed from the free energy profile as

$$\alpha = \frac{1}{1 + e^{-\beta(\Delta F_a - \Delta F_s)}} \tag{2}$$

for which we find $\alpha = 0.13 \pm 0.03$, in good agreement with other modestly polar molecules[17] though lower than previously estimated experimentally for N_2O_5.[58]

As gaseous uptake couples thermodynamics and kinetics, we have also characterized the dynamical processes of N_2O_5 as it moves between phases across the liquid-vapor interface. Before considering the rare events of evaporation and solvation, we first discuss the diffusive properties of N_2O_5 in the bulk liquid. With a simulation of N_2O_5 immersed in a bulk liquid containing 272 water molecules, we have estimated the self-diffusivity of N_2O_5 by computing mean-squared displacements[59]. The value obtained for the self-diffusion constant of N_2O_5 derived from the average mean-squared displacement was $(1.53 \pm 0.06) \times 10^{-5}$ cm^2/s. Hydrodynamic effects are known to suppress the diffusion constant for finite systems employing periodic boundary conditions.[60] Using the known experimental viscosity of liquid water at ambient conditions,[29] we can correct for these finite size effects resulting in a diffusion constant in the thermodynamic limit of $(1.89 \pm 0.06) \times 10^{-5}$ cm^2/s. We have also estimated the change in the diffusion constant at the liquid vapor interface,[61] and find an increase from its bulk value to $(5.3 \pm 0.1) \times 10^{-5}$ cm^2/s.

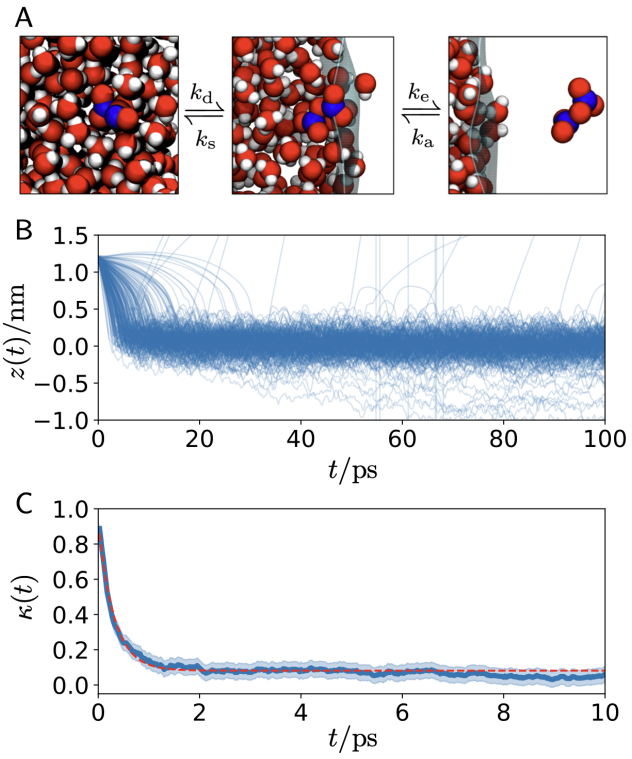

FIG. 2. Kinetics of N_2O_5 adsorption and solvation. A) Snapshots of N_2O_5. Adsorption and evaporation takes N_2O_5 between the vapor (right) and interface (center), while solvation and desolvation takes it between the interface and the bulk (left). B) Scattering trajectories following the z component of the center of mass of N_2O_5. C) Transmission coefficient for transitions between the liquid and the interface. The solid red line is an exponential fit.

Evaporation from the liquid-vapor interface and solvation into the bulk are both activated processes with barriers estimated from the free energy in Fig. 1 to be larger than typical thermal values. As such, they are rare events and difficult to sample with straightforward simulations. However, as we consider a system whose dynamics satisfies detailed balance, we can alternatively study comparatively typical events like desolvation and adsorption, and infer their reverse using the previously evaluated free energy profile.[62] Definitions for these different dynamical processes are well described in Ref. 17.

To compute the adsorption and therefore evaporation rates, we have sampled 250 scattering trajectories whereby an initially gas phase N_2O_5 placed at $z = 1.2$ nm, shown in Figure 2A, is evolved toward the liquid slab. To do this we take 10 distinct equilibrium configurations of N_2O_5 generated by constraining its center of mass to $z = 1.2$ nm, and draw 25 realizations of

a Maxwell-Boltzmann distributed velocity at 300 K for each. Figure 2B reports the trajectories of the center of mass of the N_2O_5 as it impinges on the liquid slab. Overwhelmingly, the incipient gas phase N_2O_5 molecule meets the interfaces and sticks, with only 11 out of the 250 scattering trajectories exhibiting a back scattering event, with N_2O_5 bouncing off of the interface and going back into the gas phase within the 100 ps observation time employed. The scattering rate is quantified with the so-called thermal accommodation coefficient, $S = 0.96$, relating the probability of being accommodated at the interface upon collision, consistent with previous simulations.[15] This is likely a lower bound as some of the back scattering events can be attributable to equilibration at the interface followed by subsequent evaporation. The near unity value implies a lack of a barrier to adsorption, and subsequently that evaporation is analogously limited only by the free energy of adsorption. The corresponding rates of adsorption, k_a, and evaporation, k_e, can be computed from kinetic theory.[17] Specifically, the rates are given by

$$k_a = S\frac{v}{4}, \quad k_e = k_a e^{\beta \Delta F_a} \tag{3}$$

where $v = \sqrt{8/\beta\pi m}$ is the average molecular speed of N_2O_5. These are $k_a = 57$ nm/ns and $k_e = 0.11$ nm/ns.

We have also computed the rates of solvation and desolvation following the Bennet-Chandler approach.[63] Identifying $z^\dagger = -0.42$ nm as the location of the putative transition state for solvation into the bulk liquid from the interface (see Figure 1C), we can estimate the rate of solvation and analogously desolvation by computing the transmission coefficient, κ, for committing to the interface conditioned on starting at the transition state. The transmission coefficient is defined as[63]

$$\kappa(t) = \frac{\langle v(0)\Theta(z(t) - z^\dagger)\rangle_{z^\dagger}}{\langle |v| \rangle/2} \tag{4}$$

where Θ is the step function and the brackets denote an ensemble average where in the numerator it is conditioned on starting at the transition state. We have evaluated the transmission coefficient using 2000 trajectories. Like the scattering calculations, we have taken 80 different equilibrium configurations of N_2O_5 at $z = z^\dagger$, and compose 25 Maxwell-Boltzmann velocity distributions at 300 K for each. Each trajectory was evolved for 10 ps. Fig. 2C shows that κ decays to 0.08 over 1 ps, consistent with a diffusive barrier crossing. From the plateau we can estimate the rates to solvate into the bulk, k_s, and desolvate into the interface, k_d, as

$$k_d = \kappa \frac{v}{2\ell} e^{\beta \Delta F_b}, \quad k_s = k_d \frac{\alpha}{1-\alpha} \tag{5}$$

where $\beta\Delta F_b = 0.8$ is the barrier to move from the bulk liquid to the interface and $\ell = 0.06$nm is the width of the interface.[64] We find $k_d = 340$/ns and $k_s = 47$/ns.

Experimentally, N_2O_5 undergoes facile irreversible hydrolysis with water and this reaction ultimately determines the reactive uptake in aqueous aerosol. While we cannot simulate the reactive event with the MB-nrg potential employed directly, we can still make an inference into the reactive uptake. Using the thermodynamic and kinetic parameters evaluated from the molecular dynamics simulations, we can parameterize a molecularly detailed reaction diffusion equation. Specifically, we consider the diffusive dynamics accompanying an initially adsorbed N_2O_5 molecule as it enters the bulk liquid or evaporates, and address what would happen if it were able to also undergo hydrolysis.

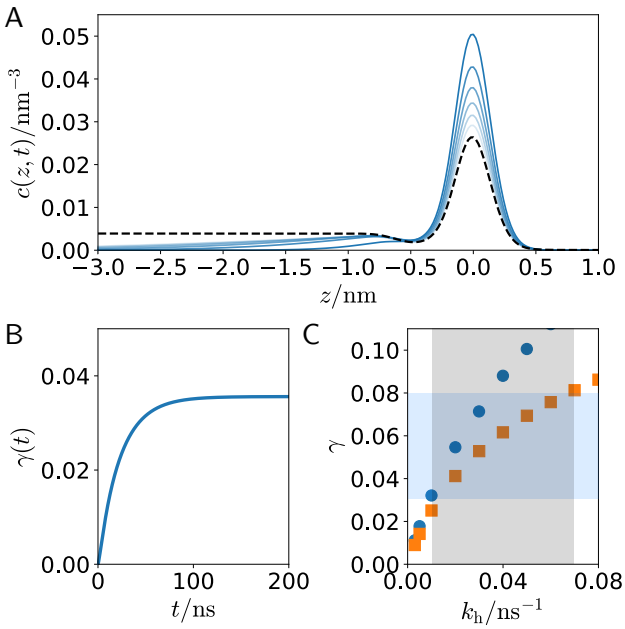

FIG. 3. Reactive uptake from the reaction-diffusion equation. A) Relaxation of the initial concentration profile. Blue lines are $c(z,t)$ separated by 0.25 ns and the dashed black line is the equilibrium profile computed from $\exp[-\beta\Delta F(z)]$. B) An example time dependent reactive uptake coefficient. Both A) and B) is computed with $k_h = 0.02$ ns^{-1} and the interfacial rate equal to $k_h/5$. C) Asymptotic uptake coefficients without (orange squares) and with (blue circles) interfacial reactivity. Blue regions denote the range of uptake coefficients observed experimentally on pure water, and grey the corresponding likely range of bulk hydrolysis rates.

Consistent with the near unity thermal accommodation S, we assume an initially adsorbed molecule locally equilibrated at the interface. The subsequent evolution of its concentration profile, $c(z,t)$, can be solved for using a Smoluchowski equation[65] of the form,

$$\begin{aligned}\frac{\partial c(z,t)}{\partial t} =& \frac{\partial}{\partial z} D(z) e^{-\beta \Delta F(z)} \frac{\partial}{\partial z} e^{\beta \Delta F(z)} c(z,t) \\ & - k_h(z) c(z,t)\end{aligned} \tag{6}$$

where $\Delta F(z)$ is the free energy profile from Fig. 1C, $D(z)$ is the diffusion constant, and $k_h(z)$ is the unknown hydrolysis rate, both of which in principle vary through space.[66,67] The first term is a drift diffusion encoding the stationary distribution implied by the free energy

profile,[68] while the second accounts for loss due to reaction. This equation is valid only for the liquid and interface, not the vapor, since it is overdamped.[65] In order to model the vapor, we employ absorbing boundary conditions $c(z = 1\,\mathrm{nm}, t) = 0$, and consider a domain that extends deeply enough into the liquid that the results are insensitive to the reflecting boundary condition employed there $\partial_z c(z = -30\,\mathrm{nm}, t) = 0$. We solve Eq. 6 with a normalized Gaussian initial condition, localized in the free energy minima near the Gibbs dividing surface where a standard deviation of 0.05 nm was found to well approximate the curvature of the interfacial minima. In practice, we employ a simple finite difference scheme with constant grid spacing of 0.02 nm and timestep 0.018 ps.

In the absence of irreversible reactions, an initial interfacial concentration of N_2O_5 will relax through a competition between diffusion into the bulk liquid and evaporation into the vapor towards the steady-state determined by the free energy profile. Figure 3A illustrates the relaxation of this concentration profile. The initial Gaussian distribution quickly looses amplitude and a diffusive front propagates into the bulk liquid, while concentration is irreversibly lost to the vapor. The initial rates to evaporate and solvate are consistent with our explicit molecular simulation calculations. In the presence of hydrolysis, in addition to loss from evaporation, there can be loss due to reaction. Since the concentration is normalized to 1, the overall reactive uptake, γ, can be computed by the portion of the loss through the reactive channel,

$$\gamma(t) = \int_0^t dt' \int dz\, k_\mathrm{h}(z) c(z, t') \tag{7}$$

We model the hydrolysis rate as having two characteristic values, one in the bulk for $z < -0.5$ nm, denoted k_h, and one at the interface for $-0.5 < z < 0.5$ nm taken to be a fraction of the bulk value, while it is set to zero in the vapor for $z > 0.5$ nm[69]. An example time series for the reactive uptake is shown in Fig. 3B, which rises from 0 to a plateau value at times much longer than the characteristic time associated with the bulk hydrolysis rate. This asymptotic value is the reactive uptake coefficient.

The reactive uptake as a function of the bulk hydrolysis rate is shown in Fig 3C. For each bulk hydrolysis rate, we have computed γ setting the interfacial rate equal to the bulk value, and also setting it to zero. We believe these are the two likely extremes, as previous explicit calculations found that interfacial hydrolysis was suppressed relative to the bulk.[13] Experimentally, the range of reactive uptake coefficients on pure water has been reported between 0.03 and 0.08,[7–9] which is consistent with a bulk hydrolysis rate between 0.01 ns^{-1} and 0.07 ns^{-1} in Fig 3C. These rates are slower than those computed directly from a previous neural network model,[13] but faster than that typically inferred experimentally.[70] The disagreement with respect to the neural network model could likely be a failure of the density functional used in the training data, by delocalizing the charge transfer accompanying hydrolysis.[71–73] The disagreement with the rates inferred experimentally is because those are based on reactive uptake models that neglect interfacial reactivity and stability. The confirmation of the importance of the interface, reducing the diffusion into the bulk and accounting for a significant fraction of hydrolysis, agrees with the previous neural network model study,[13] and the need to revise the standard resistor model. The hydrolysis rate obtained with our modelling in addition to the other parameters relevant to reactive uptake are summarized in Table I.

TABLE I. Physical and chemical properties of N_2O_5

Henry's Law Constant	H	(3.0±0.4) M/atm
Mass Accommodation	α	0.13 ± 0.03
Diffusivity	D	$(1.89 \pm 0.06) \times 10^{-5}$ cm^2/s
Sticking Coefficient	S	0.96
Hydrolysis Rate[a]	k_h	$(4\pm3)\times10^{-2}$ ns^{-1}

[a] The range of hydrolysis rates is inferred from the solution of Eq. 6 and the known experimental range of uptake coefficients.

Apart from quantifying a likely range of experimental hydrolysis rates, the analysis of the reaction diffusion model provides insight into the likely mechanism of reactive uptake. Specifically, the range of uptake values observed upon changing the interfacial hydrolysis rate from 0 to k_h illustrates that, while interfacial reactivity contributes to the reactive uptake coefficient, it accounts for at most 20%. The interfacial contribution is lower than recent estimates,[13] due to the increased solubility predicted by the MB-nrg model and corresponding higher accommodation coefficient relative to the previous neural network model study. Nevertheless, a significant adsorption free energy reduces diffusion into the bulk liquid, resulting in an effective renormalized reaction-diffusion length. Absent barriers to solvation, the reaction diffusion length, $\ell_r = \sqrt{D/k_\mathrm{h}}$, would be around 15 nm. However, the barrier to solvation and corresponding free energy minima at the interface results in a propagation length of N_2O_5 into the bulk fluid of only around 2 nm (see Fig. 3A). This implies that reactive uptake is affected by interfacial characteristics, even though most of the reaction is predicted to take place in the bulk. It also predicts a very weak aerosol particle size dependence to reactive uptake consistent with some experimental observations.[70]

The framework and parameters determined here can be used as a new starting point for further modeling efforts to predict the reactive uptake of N_2O_5 in more complex solutions. It is well known that the reactive uptake can be modulated in the presence of inorganic salts, as in the case of excess nitrate ions.[18] Further, the branching ratios to alternative less soluble products like to $ClNO_2$ in the presence of NaCl have been well studied.[11,74] By quantifying the changes to both the thermodynamic and

kinetic properties of N_2O_5 in the presence of these alternative solutions, advanced molecular models such as the ones used in this work in combination with similar analysis of generalized reaction-diffusion equations incorporating alternative loss mechanics, can be exploited to provide a complete picture of reactive uptake of N_2O_5 with the full complexity of field measurements.

Acknowledgements We thank T. Bertram, B. Gerber, G. Nathanson and F. Paesani for stimulating discussions. This work was funded by the National Science Foundation through the National Science Foundation Center for Aerosol Impacts on Chemistry of the Environment (NSF-CAICE) under grant number CHE 1801971. This work used the Extreme Science and Engineering Discovery Environment (XSEDE), which is supported by the NSF under grant number ACI-1053575 (resources at the San Diego Supercomputer Center and the Texas Advanced Computing Center).

Supporting Information Available Figure illustrating all thermodynamic and kinetic parameters based on the free energy profile and characteristic molecular dynamics snapshots; table collecting all thermodynamic and kinetic parameters determined in this work; details on the calculation of diffusion coefficients from mean-squared displacements in the molecular dynamics simulations (PDF). Equilibrated coordinates and input files for molecular dynamics simulations, source code to solve reaction-diffusion equations, data and source code to generate all Figures (ZIP).

The data related to this publication can be accessed from the NSF-CAICE Data Repository[75] at https://doi.org/10.6075/xxx.

References

[1]T. Peter, "Microphysics and heterogeneous chemistry of polar stratospheric clouds," Annual Review of Physical Chemistry **48**, 785–822 (1997).

[2]B. J. Finlayson-Pitts and J. N. Pitts Jr, *Chemistry of the upper and lower atmosphere: theory, experiments, and applications* (Elsevier, 1999).

[3]A. Ravishankara, "Heterogeneous and multiphase chemistry in the troposphere," Science **276**, 1058–1065 (1997).

[4]U. Pöschl and M. Shiraiwa, "Multiphase chemistry at the atmosphere–biosphere interface influencing climate and public health in the anthropocene," Chemical Reviews **115**, 4440–4475 (2015).

[5]C. D. Holmes, T. H. Bertram, K. L. Confer, K. A. Graham, A. C. Ronan, C. K. Wirks, and V. Shah, "The role of clouds in the tropospheric NO_x cycle: a new modeling approach for cloud chemistry and its global implications," Geophys. Res. Lett. **46**, 4980–4990 (2019).

[6]B. Alexander, T. Sherwen, C. D. Holmes, J. A. Fisher, Q. Chen, M. J. Evans, and P. Kasibhatla, "Global inorganic nitrate production mechanisms: comparison of a global model with nitrate isotope observations," Atmospheric Chemistry and Physics **20**, 3859–3877 (2020).

[7]J. Davis, P. Bhave, and K. Foley, "Parameterization of N_2O_5 reaction probabilities on the surface of particles containing ammonium, sulfate, and nitrate," Atmos. Chem. Phys **8**, 5295–5311 (2008).

[8]J. A. Thornton and J. P. Abbatt, "N_2O_5 reaction on submicron sea salt aerosol: Kinetics, products, and the effect of surface active organics," J. Phys. Chem. A **109**, 10004–10012 (2005).

[9]W. L. Chang, P. V. Bhave, S. S. Brown, N. Riemer, J. Stutz, and D. Dabdub, "Heterogeneous atmospheric chemistry, ambient measurements, and model calculations of N_2O_5: A review," Aerosol Sci. Technol. **45**, 665–695 (2011).

[10]E. E. McDuffie, D. L. Fibiger, W. P. Dubé, F. Lopez-Hilfiker, B. H. Lee, J. A. Thornton, V. Shah, L. Jaeglé, H. Guo, R. J. Weber, *et al.*, "Heterogeneous N_2O_5 uptake during winter: Aircraft measurements during the 2015 winter campaign and critical evaluation of current parameterizations," J. Geophys. Res. D: Atmos. **123**, 4345–4372 (2018).

[11]N. V. Karimova, J. Chen, J. R. Gord, S. Staudt, T. H. Bertram, G. M. Nathanson, and R. B. Gerber, "SN_2 reactions of N_2O_5 with ions in water: Microscopic mechanisms, intermediates, and products," The Journal of Physical Chemistry A **124**, 711–720 (2019).

[12]L. M. McCaslin, M. A. Johnson, and R. B. Gerber, "Mechanisms and competition of halide substitution and hydrolysis in reactions of N_2O_5 with seawater," Science Advances **5**, eaav6503 (2019).

[13]M. Galib and D. T. Limmer, "Reactive uptake of N_2O_5 by atmospheric aerosol is dominated by interfacial processes," Science **371**, 921–925 (2021).

[14]C. E. Kolb, R. A. Cox, J. P. D. Abbatt, M. Ammann, E. J. Davis, D. J. Donaldson, B. C. Garrett, C. George, P. T. Griffiths, D. R. Hanson, M. Kulmala, G. McFiggans, U. Pöschl, I. Riipinen, M. J. Rossi, Y. Rudich, P. E. Wagner, P. M. Winkler, D. R. Worsnop, and C. D. O' Dowd, "An overview of current issues in the uptake of atmospheric trace gases by aerosols and clouds," Atmospheric Chemistry and Physics **10**, 10561–10605 (2010).

[15]B. Hirshberg, E. R. Molina, A. W. Götz, A. D. Hammerich, G. M. Nathanson, T. H. Bertram, M. A. Johnson, and R. B. Gerber, "N_2O_5 at water surfaces: binding forces, charge separation, energy accommodation and atmospheric implications," Phys. Chem. Chem. Phys. **20**, 17961–17976 (2018).

[16]V. W. D. Cruzeiro, E. Lambros, M. Riera, R. Roy, F. Paesani, and A. W. Götz, "Highly accurate many-body potentials for simulations of N_2O_5 in water: Benchmarks, development, and validation," Journal of Chemical Theory and Computation (2021).

[17]P. Davidovits, C. E. Kolb, L. R. Williams, J. T. Jayne, and D. R. Worsnop, "Mass accommodation and chemical reactions at gas-liquid interfaces," Chemical Reviews **106**, 1323–1354 (2006).

[18]T. H. Bertram, J. A. Thornton, T. P. Riedel, A. M. Middlebrook, R. Bahreini, T. S. Bates, P. K. Quinn, and D. J. Coffman, "Direct observations of N_2O_5 reactivity on ambient aerosol particles," Geophysical Research Letters **36** (2009).

[19]M. von Domaros, P. S. Lakey, M. Shiraiwa, and D. J. Tobias, "Multiscale modeling of human skin oil-induced indoor air chemistry: Combining kinetic models and molecular dynamics," The Journal of Physical Chemistry B **124**, 3836–3843 (2020).

[20]M. A. Wilson and A. Pohorille, "Adsorption and solvation of ethanol at the water liquid- vapor interface: a molecular dynamics study," The Journal of Physical Chemistry B **101**, 3130–3135 (1997).

[21]R. S. Taylor and B. C. Garrett, "Accommodation of alcohols by the liquid/vapor interface of water: Molecular dynamics study," The Journal of Physical Chemistry B **103**, 844–851 (1999).

[22]E. Rossich Molina and R. B. Gerber, "Microscopic mechanisms of N_2O_5 hydrolysis on the surface of water droplets," The Journal of Physical Chemistry A **124**, 224–228 (2019).

[23]G. A. Cisneros, K. T. Wikfeldt, L. OjamaÌĹe, J. Lu, Y. Xu, H. Torabifard, A. P. Bartók, G. Csányi, V. Molinero, and F. Paesani, "Modeling molecular interactions in water: From pairwise to many-body potential energy functions," Chemical Reviews **116**, 7501–7528 (2016).

[24]F. Paesani, "Getting the right answers for the right reasons: Toward predictive molecular simulations of water with many-body potential energy functions," Accounts of Chemical Research **49**, 1844–1851 (2016).

[25]S. N. Niblett, M. Galib, and D. T. Limmer, "Learning intermolecular forces at liquid-vapor interfaces," arXiv:2107.06208 (2021).

[26]V. Babin, C. Leforestier, and F. Paesani, "Development of a "first principles" water potential with flexible monomers: Dimer potential energy surface, vrt spectrum, and second virial coefficient," Journal of Chemical Theory and Computation **9**, 5395–5403 (2013).

[27]V. Babin, G. R. Medders, and F. Paesani, "Development of a "first principles" water potential with flexible monomers. ii: Trimer potential energy surface, third virial coefficient, and small clusters," Journal of Chemical Theory and Computation **10**, 1599–1607 (2014), pMID: 26580372.

[28]G. R. Medders, V. Babin, and F. Paesani, "Development of a "first-principles" water potential with flexible monomers. III. Liquid phase properties," Journal of Chemical Theory and Computation **10**, 2906–2910 (2014).

[29]S. K. Reddy, S. C. Straight, P. Bajaj, C. Huy Pham, M. Riera, D. R. Moberg, M. A. Morales, C. Knight, A. W. Götz, and F. Paesani, "On the accuracy of the mb-pol many-body potential for water: Interaction energies, vibrational frequencies, and classical thermodynamic and dynamical properties from clusters to liquid water and ice," The Journal of Chemical Physics **145**, 194504 (2016).

[30]G. R. Medders and F. Paesani, "Infrared and raman spectroscopy of liquid water through âĂIJfirst-principlesâĂİ many-body molecular dynamics," Journal of Chemical Theory and Computation **11**, 1145–1154 (2015), pMID: 26579763.

[31]G. R. Medders and F. Paesani, "Dissecting the molecular structure of the air/water interface from quantum simulations of the sum-frequency generation spectrum," Journal of the American Chemical Society **138**, 3912–3919 (2016), pMID: 26943730.

[32]S. C. Straight and F. Paesani, "Exploring electrostatic effects on the hydrogen bond network of liquid water through many-body molecular dynamics," The Journal of Physical Chemistry B **120**, 8539–8546 (2016), pMID: 27109247.

[33]S. E. Brown, A. W. Götz, X. Cheng, R. P. Steele, V. A. Mandelshtam, and F. Paesani, "Monitoring water clusters âĂIJmeltâĂİ through vibrational spectroscopy," Journal of the American Chemical Society **139**, 7082–7088 (2017), pMID: 28464604.

[34]C. H. Pham, S. K. Reddy, K. Chen, C. Knight, and F. Paesani, "Many-body interactions in ice," Journal of Chemical Theory and Computation **13**, 1778–1784 (2017), pMID: 28245359.

[35]D. R. Moberg, S. C. Straight, C. Knight, and F. Paesani, "Molecular origin of the vibrational structure of ice ih," The Journal of Physical Chemistry Letters **8**, 2579–2583 (2017), pMID: 28541703.

[36]S. K. Reddy, D. R. Moberg, S. C. Straight, and F. Paesani, "Temperature-dependent vibrational spectra and structure of liquid water from classical and quantum simulations with the mb-pol potential energy function," The Journal of Chemical Physics **147**, 244504 (2017).

[37]K. M. Hunter, F. A. Shakib, and F. Paesani, "Disentangling coupling effects in the infrared spectra of liquid water," The Journal of Physical Chemistry B **122**, 10754–10761 (2018), pMID: 30403350.

[38]D. R. Moberg, S. C. Straight, and F. Paesani, "Temperature dependence of the air/water interface revealed by polarization sensitive sum-frequency generation spectroscopy," The Journal of Physical Chemistry B **122**, 4356–4365 (2018), pMID: 29614228.

[39]D. R. Moberg, P. J. Sharp, and F. Paesani, "Molecular-level interpretation of vibrational spectra of ordered ice phases," The Journal of Physical Chemistry B **122**, 10572–10581 (2018), pMID: 30358400.

[40]A. P. Gaiduk, T. A. Pham, M. Govoni, F. Paesani, and G. Galli, "Electron affinity of liquid water," Nature Communications **9**, 247 (2018).

[41]Z. Sun, L. Zheng, M. Chen, M. L. Klein, F. Paesani, and X. Wu, "Electron-hole theory of the effect of quantum nuclei on the x-ray absorption spectra of liquid water," Phys. Rev. Lett. **121**, 137401 (2018).

[42]D. R. Moberg, D. Becker, C. W. Dierking, F. Zurheide, B. Bandow, U. Buck, A. Hudait, V. Molinero, F. Paesani, and T. Zeuch, "The end of ice I," Proceedings of the National Academy of Sciences **116**, 24413–24419 (2019), https://www.pnas.org/content/116/49/24413.full.pdf.

[43]V. W. D. Cruzeiro, A. Wildman, X. Li, and F. Paesani, "Relationship between hydrogen-bonding motifs and the 1b1 splitting in the x-ray emission spectrum of liquid water," The Journal of Physical Chemistry Letters **12**, 3996–4002 (2021), pMID: 33877847.

[44]F. Paesani, P. Bajaj, and M. Riera, "Chemical accuracy in modeling halide ion hydration from many-body representations," Advances in Physics: X **4**, 1631212 (2019).

[45]M. Riera, N. Mardirossian, P. Bajaj, A. W. Götz, and F. Paesani, "Toward chemical accuracy in the description of ion–water interactions through many-body representations. alkali-water dimer potential energy surfaces," The Journal of Chemical Physics **147**, 161715 (2017).

[46]P. Bajaj, A. W. Götz, and F. Paesani, "Toward chemical accuracy in the description of ionâĂŞwater interactions through many-body representations. I. HalideâĂŞwater dimer potential energy surfaces," Journal of Chemical Theory and Computation **12**, 2698–2705 (2016), pMID: 27145081.

[47]M. Riera, E. P. Yeh, and F. Paesani, "Data-driven many-body models for molecular fluids: CO_2/H_2O mixtures as a case study," Journal of Chemical Theory and Computation **16**, 2246–2257 (2020).

[48]M. Riera, A. Hirales, R. Ghosh, and F. Paesani, "Data-driven many-body models with chemical accuracy for CH_4/H_2O mixtures," The Journal of Physical Chemistry B **124**, 11207–11221 (2020).

[49]D. Bedeaux and J. D. Weeks, "Correlation functions in the capillary wave model of the liquid–vapor interface," The Journal of Chemical Physics **82**, 972–979 (1985).

[50]D. A. Case, K. Belfon, I. Y. Ben-Shalom, S. R. Brozell, D. S. Cerutti, I. Cheatham, T. E., V. W. D. Cruzeiro, T. A. Darden, R. E. Duke, G. Giambasu, M. K. Gilson, H. Gohlke, A. W. Goetz, R. Harris, S. Izadi, S. A. Izmailov, K. Kasavajhala, A. Kovalenko, R. Krasny, T. Kurtzman, T. S. Lee, S. LeGrand, P. Li, C. Lin, J. Liu, T. Luchko, R. Luo, V. Man, K. M. Merz, Y. Miao, O. Mikhailovskii, G. Monard, H. Nguyen, A. Onufriev, F. Pan, S. Pantano, R. Qi, D. R. Roe, A. Roitberg, C. Sagui, S. Schott-Verdugo, J. Shen, C. Simmerling, N. R. Skrynnikov, J. Smith, J. Swails, R. C. Walker, J. Wang, L. Wilson, R. M. Wolf, X. Wu, Y. Xiong, Y. Xue, D. M. York, and P. A. Kollman, "AMBER 2020," (2020).

[51]"MBX: A many-body energy and force calculator," `http://paesanigroup.ucsd.edu/software/mbx.html`.

[52]D. Frenkel and B. Smit, *Understanding molecular simulation: from algorithms to applications*, Vol. 1 (Elsevier, 2001).

[53]J. Kästner and W. Thiel, "Bridging the gap between thermodynamic integration and umbrella sampling provides a novel analysis method:"umbrella integration"," The Journal of Chemical Physics **123**, 144104 (2005).

[54]The free energy profile along with an overview of all thermodynamic and kinetic parameters discussed in this text is contained in the Supporting Information.

[55]W. Li, C. Y. Pak, and Y.-L. S. Tse, "Free energy study of H_2O, N_2O_5, SO_2, and O_3 gas sorption by water droplets/slabs," The Journal of Chemical Physics **148**, 164706 (2018).

[56]R. Sander, "Compilation of Henry's law constants (version 4.0) for water as solvent," Atmospheric Chemistry and Physics **15**, 4399–4981 (2015).

[57]T. F. Mentel, M. Sohn, and A. Wahner, "Nitrate effect in the heterogeneous hydrolysis of dinitrogen pentoxide on aqueous aerosols," Physical Chemistry Chemical Physics **1**, 5451–5457 (1999).

[58]G. Gržinić, T. Bartels-Rausch, A. Türler, and M. Ammann, "Efficient bulk mass accommodation and dissociation of N_2O_5 in neutral aqueous aerosol," Atmospheric Chemistry and Physics **17**, 6493–6502 (2017).

[59]Further details about our protocol are discussed at the Support-

ing Information.
[60]I.-C. Yeh and G. Hummer, "System-size dependence of diffusion coefficients and viscosities from molecular dynamics simulations with periodic boundary conditions," The Journal of Physical Chemistry B **108**, 15873–15879 (2004).
[61]G. Hummer, "Position-dependent diffusion coefficients and free energies from Bayesian analysis of equilibrium and replica molecular dynamics simulations," New Journal of Physics **7**, 34 (2005).
[62]P. Varilly and D. Chandler, "Water evaporation: A transition path sampling study," The Journal of Physical Chemistry B **117**, 1419–1428 (2013).
[63]D. Chandler, "Statistical mechanics of isomerization dynamics in liquids and the transition state approximation," The Journal of Chemical Physics **68**, 2959–2970 (1978).
[64]The width of the interface is determined by fitting the free energy minima to a parabola and integrating the resultant Gaussian distribution from $1nm > z > z^{\dagger}$.
[65]R. Zwanzig, *Nonequilibrium statistical mechanics* (Oxford University Press, 2001).
[66]A. J. Schile and D. T. Limmer, "Rate constants in spatially inhomogeneous systems," The Journal of Chemical Physics **150**, 191102 (2019).
[67]S. P. Niblett and D. T. Limmer, "Ion dissociation dynamics in an aqueous premelting layer," The Journal of Physical Chemistry B **125**, 2174–2181 (2021).
[68]In practice we fit the free energy to an analytic function form, $\beta\Delta F(z) = a_1 \tanh[(z - a_2)/a_3] - a_4 \exp[-(z - a_5)^2/a_6] + a_7 \exp[-(z - a_8)^2/a_9]$.
[69]The interfacial region was determined from the inflection points in the free energy curve. Numerical tests have shown that the results are insensitive to the precise width of the interfacial region.
[70]C. J. Gaston and J. A. Thornton, "Reacto-diffusive length of N_2O_5 in aqueous sulfate- and chloride-containing aerosol particles," The Journal of Physical Chemistry A **120**, 1039–1045 (2016).
[71]A. J. Cohen, P. Mori-Sánchez, and W. Yang, "Challenges for density functional theory," Chemical Reviews **112**, 289–320 (2012).
[72]N. Mardirossian and M. Head-Gordon, "Thirty years of density functional theory in computational chemistry: an overview and extensive assessment of 200 density functionals," Molecular Physics **115**, 2315–2372 (2017).
[73]S. Mandal, J. Debnath, B. Meyer, and N. N. Nair, "Enhanced sampling and free energy calculations with hybrid functionals and plane waves for chemical reactions," The Journal of Chemical Physics **149**, 144113 (2018).
[74]J. M. Roberts, H. D. Osthoff, S. S. Brown, A. Ravishankara, D. Coffman, P. Quinn, and T. Bates, "Laboratory studies of products of N_2O_5 uptake on Cl^- containing substrates," Geophysical Research Letters **36** (2009).
[75]V. W. D. Cruzeiro, M. Galib, D. T. Limmer, and A. W. Götz, "Data from: Insights Into the Uptake of N_2O_5 by Aqueous Aerosol Using Chemically Accurate Many-Body Potentials," Center for Aerosol Impact on Chemistry of the Environment (CAICE). UC San Diego Library Digital Collections (2021).